Available online at www.sciencedirect.com
ScienceDirect
Trans. Nonferrous Met. Soc. China 19(2009) 1180−1184
Transactions of Nonferrous Metals Society of China
www.tnmsc.cn

Microstructure and properties of TiN/Ni composite coating prepared by plasma transferred arc scanning process

WANG Wei(王 伟), QIAN Shi-qiang(钱士强), ZHOU Xi-ying(周细应)

School of Materials Engineering, Shanghai University of Engineering Science, Shanghai 201620, China

Received 1 September 2008; accepted 13 March 2009

Abstract: The TiN/Ni composite coatings were deposited on 7005 aluminium alloy by high speed jet electroplating and then processed with plasma transferred arc(PTA) scanning process. The microstructure, microhardness and friction coefficient of PTA scanning treated specimens were investigated. It is shown that the PTA scanning treated specimens have a rapidly solidified microstructure consisting of the uniformly distributed TiN phase and fine Al_3Ni_2 intermetallic phases. The composite coating has an average microhardness of approximately HV 800. The friction coefficient of PTA scanning treated specimens (oscillated at around 0.25) is considerably lower than that of TiN/Ni composite coating (oscillated at around 0.35). The corrosion behavior of the composite coating in 3.5% NaCl solution at room temperature was also determined using a potentiostat system. In comparison with the corrosion potential φ_{corr} of −0.753 V for 7005 aluminium alloy, the corrosion potentials for TiN/Ti composite coating and PTA scanning treated specimen are increased by 0.148 V and 0.305 V, respectively. The PTA scanning treated specimen has the lowest corrosion current density J_{corr} as well as the highest corrosion potential φ_{corr}, showing an improved corrosion resistance compared with 7005 aluminium alloy.

Key words: plasma transferred arc; TiN/Ni; friction coefficient; microstructure; corrosion resistance

1 Introduction

Aluminum alloys are becoming increasingly important, especially in the automotive and aerospace industries. However, these materials tend to have poor wear and corrosion resistance[1−2]. TiN ceramic coatings are potentially effective in developing hard, wear- and corrosion-resistant surfaces[3−5]. Nevertheless, coatings applied to aluminum alloys, by traditional processes such as hard anodizing or thermal spaying, have suffered from the low support from the underlying material and insufficient adhesion, which reduces their durability[6−9].

Composite electroplating, with ceramic particles as second phases in the metal matrix, is a typical surface modification process for improving wear and corrosion resistance[10−11]. In contrast to the conventional electrodeposition, high speed jet electroplating as a high speed electroplating technique with special flow characteristics has been used for local coating reaction on an unmasked cathode[12−13]. However, the composite coatings produced by high speed jet electroplating are mechanically bonded with substrate, making that the coating cannot bear aggressive attack.

The plasma transferred arc(PTA) is a kind of constricted arc with high energy density and high temperature. It is widely used in the traditional metal processes, such as plasma spray and plasma cutting. The PTA process, compared with laser process, is easy to operate. The cost of PTA equipment is lower than that of the laser equipment. Therefore, PTA is often used as a heating source to prepare new types of materials[14−15].

In the present study, the TiN/Ni composite coatings were deposited on 7005 aluminium alloy by high speed jet electroplating and then processed with PTA scanning. The microstructure of the composite coatings was characterized. The microhardness, friction property and corrosion resistance of the composite coatings were discussed.

2 Experimental

7005 aluminium alloy of the following compositions

Foundation item: Project(0852nm01400) supported by Shanghai Municipal Developing Foundation of Science and Technology, China; Project(XK0706) supported by the Leading Academic Discipline of Shanghai Education Commission, China

Corresponding author: WANG Wei; Tel: +86-21-67791203; E-mail: wangwei200173@sina.com

DOI: 10.1016/S1003-6326(08)60425-2

was used as substrate material (mass fraction): 0.25% Si, 0.24% Fe, 0.08% Cu, 0.43% Mn, 1.33% Mg, 4.59% Zn, 0.03% Ti, 0.13% Cr, 0.13% Zr, and balance Al. Specimens in the form of plates with dimensions of 20 mm×20 mm×2 mm were cut and polished to a mirror finish with 1 μm Al_2O_3 power, then degreased by detergent and further ultrasonically cleaned in deionized water and acetone, at last dried by N_2 gas. Prior to jet electroplating, the substrates were pretreated through an electroless Zn-Al coating to counteract the poor adhesion of deposits caused by an oxide film on aluminium alloy substrate. As incorporated ceramic reinforcements, TiN particles with an average diameter of 30−40 nm were adopted.

The TiN/Ni composite coatings were prepared through co-depositing TiN particles and pure nickel on 7005 aluminium alloy substrate by high speed jet electroplating technique. Before jet electroplating, a mechanical method, ultrasonic and surfactant (sodium laurylsulfate) were used to make TiN particles uniformly suspended in a nickel jet electroplating electrolyte as soon as possible. The basic composition of the electrolyte bath and conditions of high speed jet electroplating are listed in Table 1. The PTA process was performed using a LHM−315IGBT apparatus. The deposition conditions for PTA welding used in this study are listed in Table 2.

The microstructural characterization of the composite coatings was carried out by X-ray diffractometry(XRD), optical microscopy(OM) and scanning electron microscopy(SEM).

The Vickers microhardness was measured by microhardness tester (HX−1000) with a load of 0.98 N for 15 s. Scratch tests were made using MTS Nano Indenter® XP scratch tester. To obtain friction coefficients, a constant-load scratch test was performed. The scratch length, scratch velocity and scratch force were 500 μm, 10 μm/s and 50 mN, respectively. The coefficient of friction, μ, is expressed by the equation, $\mu=P_T/P_N$, where P_N is the applied normal force for indentation and P_T is the tangential force.

Anodic polarization curves were obtained using a potentiostat system (EG&G Model 273A Potentiostat/ Galvanostat). The 3.5% NaCl solution was kept at room temperature of 23 ℃ and deaerated by purging with nitrogen gas for 1 h prior to corrosion tests. A saturated calomel electrode(SCE) was used as the reference electrode and two parallel graphite rods served as the counter electrode for current measurement. To avoid crevice corrosion, protective tape was used to mask samples, allowing 0.25 cm^2 of the surface to be in contact with the solution. Specimens were immersed in the solution for 2 h before testing. Anodic polarization curves were recorded between −400 and +750 mV over the corrosion potential at a scan rate of 1 mV/s.

Table 1 Bath composition and electroplating conditions

Item	Value
$\rho(NiSO_4\cdot 6H_2O)/(g\cdot L^{-1})$	260
$\rho((NH_4)_3C_6H_5O_7)/(g\cdot L^{-1})$	50
ρ(Ammonia)/(g·L^{-1})	150
Bath temperature/℃	45
pH	7
Jet speed/(L·h^{-1})	360
Scanning jet speed/(mm·s^{-1})	6
Jet voltage/V	8
Jet time/min	15
ρ(TiN)/(g·L^{-1})	6

Table 2 PTA process parameters

Item	Value
Arc current/A	20
Arc voltage/V	18
Shield gas flow(Ar)/(L·min^{-1})	7
Plasma gas flow(Ar)/(L·min^{-1})	1.6
Travel speed/(mm·s^{-1})	5
Powder feed rate/(g·s^{-1})	0.134

3 Results and discussion

3.1 Microstructure

Fig.1 shows cross-section SEM micrograph of TiN/Ni composite coatings deposited on 7005 aluminium alloy by high speed jet electroplating. A relatively smooth surface was observed on the composite coatings of 6 μm in thickness. Furthermore, it can also be seen that a dense and crack-free TiN/Ni composite coatings are obtained. In Fig.1, the interface between the

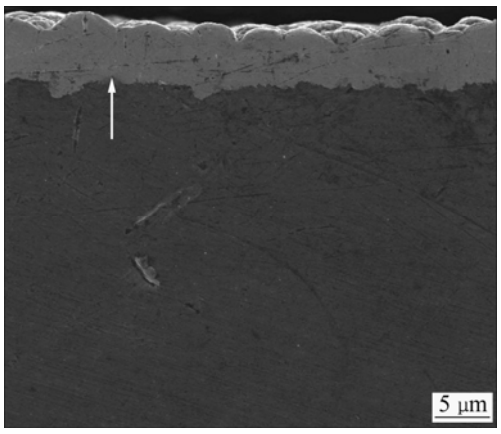

Fig.1 Cross-section SEM micrograph of TiN/Ni composite coatings before PTA scanning

composite coating and the substrate is close to a straight line.

Fig.2 presents a cross-sectional morphology of 7005 aluminium alloy covered with the PTA scanning treated TiN/Ni composite coating. It can also be found out that the sample exhibits three regions: the fusion zone that underwent melting and solidification, the heat-affected zone and the base-metal zone which was unaffected by the PTA scanning. This indicates that the PTA scanning can lead to a reduction in overlay porosity and an increase in composite coating adhesion. The PTA scanning treated TiN/Ni composite coating is metallurgically bonded to the 7005 aluminium alloy substrate.

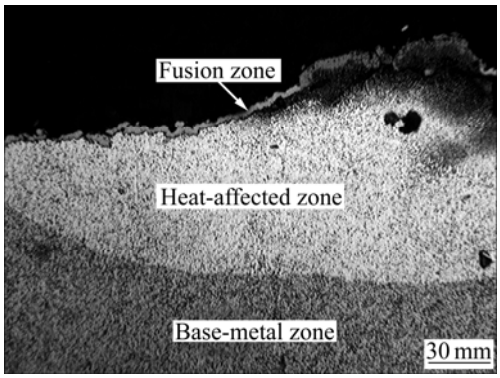

Fig.2 Cross-sectional morphology of PTA scanning treated specimen

Fig.3 shows the XRD patterns of the TiN/Ni composite coating. The XRD pattern of TiN/Ni composite coating without PTA scanning principally consists of two phases, namely, pure Ni and TiN (Fig.3(a)). After PTA scanning, it is mainly composed of pure Ni, TiN and Al_3Ni_2 phases (Fig.3(b)). The presence of Al_3Ni_2 intermetallic phase is attributed to rapid solidification occurring in PTA scanning that leads to a non-equilibrium reaction.

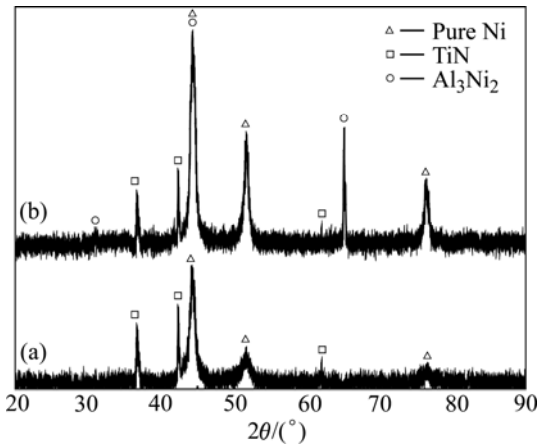

Fig.3 X-ray patterns of TiN/Ni composite coating before (a) and after (b) PTA scanning

Fig.4 shows the microstructures of the fusion zone and the substrate of the PTA scanning treated specimen. There are many oriented dendrites and columnar grains between the composite coating and the substrate. The small orientated columnar grains are intergrown into the substrate, which leads to a good metallurgical bond at the composite coating/substrate interface. The substrate consists of coarse dendrites (α(Al)) and eutectics. The microstructures in the composite coatings are much finer than those in substrate due to rapid quenching process.

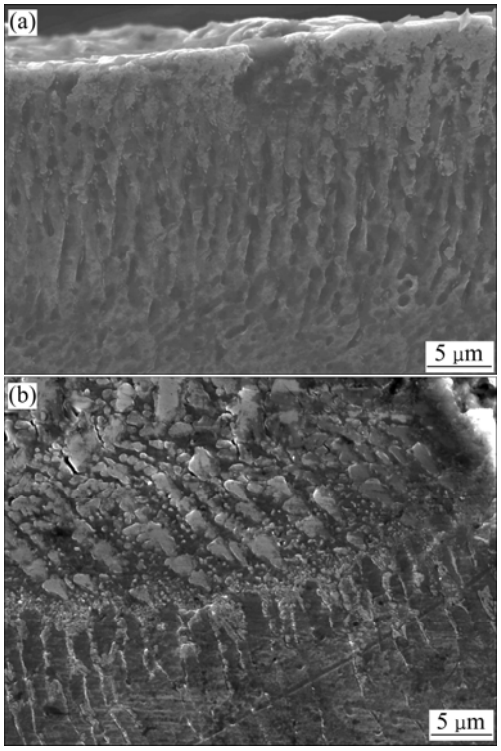

Fig.4 Cross-sectional SEM images of fusion zone (a) and substrate (b) of PTA scanning treated specimen

3.2 Microhardness

Fig.5 indicates the microhardness profile along the depth direction of the PTA scanning treated TiN/Ni composite coating. It can be observed that the 7005 aluminium alloy has an average microhardness of approximately HV 118. Because of the presence of the hard TiN dendrites and Al_3Ni_2 intermetallic phase, the composite coating has an average microhardness of approximately HV 800 and uniform microhardness distribution within the composite coatings except in the composite coating/substrate bonding zone, where the microhardness decreases gradually to the substrate.

A constant-load scratch technique was employed in order to investigate the frictional behavior of the composite coatings. Fig.6 shows the friction coefficient—scratch distance curves of TiN/Ni composite coating and PTA scanning treated specimen. The coefficient of friction indicates the resistance of the

material to tip penetration in the tangential direction, which is determined from the ratio of the force to the normal force. The friction coefficient of PTA scanning treated specimen (oscillating at around 0.25) is considerably lower than that of TiN/Ni composite coating (oscillating at around 0.35). It can be concluded that the PTA scanning treated TiN/Ni composite coating has excellent friction property. This may be attributed to the higher microhardness of the PTA scanning treated TiN/Ni composite coating, resulting in lower real area of contact, therefore, smaller number of junctions require less energy to get sheared during sliding as compared with the TiN/Ni composite coating.

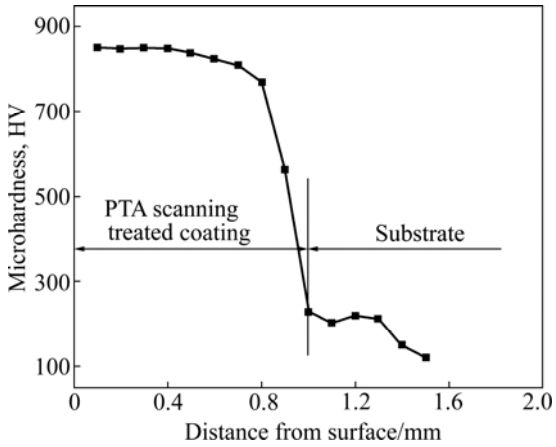

Fig.5 Microhardness profile on cross-section of PTA scanning treated specimen

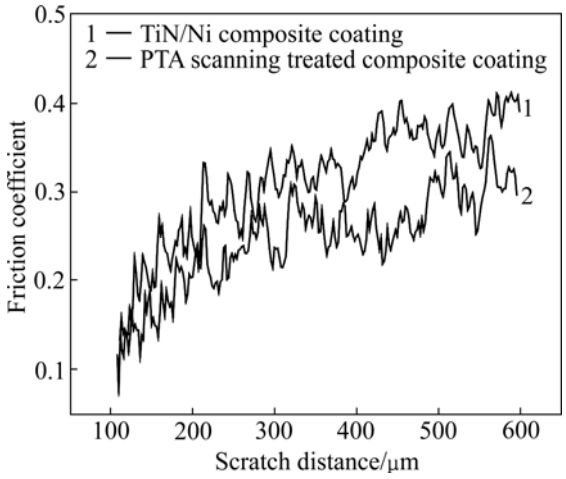

Fig.6 Friction coefficient as function of scratch distance

3.3 Electrochemical corrosion behaviour

Fig.7 illustrates the polarization curves of potential (vs SCE) against current density of specimens, carried out in 3.5% NaCl solution. Corrosion parameters, such as the corrosion current density(J_{corr}) and the corrosion potential(φ_{corr}), are estimated from Tafel plots by extrapolating the cathodic and anodic branches back to common points.

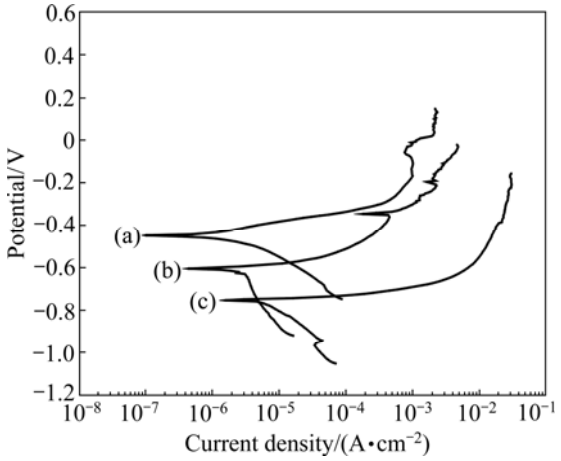

Fig.7 Anodic polarization curves of substrates (7005 aluminium alloy) (a), TiN/Ni composite coating (b) and PTA scanning treated specimen (c)

As shown in Fig.7, in comparison with the corrosion potential φ_{corr} of −0.753 V for 7005 aluminium alloy, the corrosion potential φ_{corr} for TiN/Ti composite coating and PTA scanning treated specimen is increased by 0.148 V and 0.305 V, respectively. Fig.7 shows that the PTA scanning treated specimen has the lowest corrosion current density J_{corr} as well as the highest corrosion potential φ_{corr}. This indicates that the PTA scanning can greatly improve the corrosion resistance of the composite coating. It can also be found out that the sample after PTA scanning exhibits a passive region which possesses a lower passive current density. It can be attributed to the fact that PTA scanning can induce the formation of uniformly distributed fine Al_3Ni_2 intermetallic particles (Fig.4).

TiN particles appear to act as cathodic sites in the composite coating, accelerating localized dissolution of the aluminium matrix to some extent. After PTA scanning, Al_3Ni_2 intermetallic phase is formed on the surface of the TiN particles (Fig.3), and these particles can behave in a highly anodic manner towards the aluminium matrix[16].

4 Conclusions

1) A new technique combining PTA and high speed jet electroplating TiN/Ni composite coating has been demonstrated to be successful.

2) The PTA scanning treated TiN/Ni composite coating is metallurgically bonded to the 7005 aluminium alloy substrate.

3) The microhardness of the PTA scanning treated TiN/Ni composite coating is about HV 852 and is seven times higher than that of the 7005 aluminium alloy substrate (about HV 118), which is due to the formation of hard TiN and Al_3Ni_2 intermetallic phases.

4) In comparison with the friction coefficient of 0.35 for TiN/Ni composite coating, the friction coefficient for PTA scanning treated specimen is dropped to 0.25. The PTA scanning can also greatly improve the corrosion resistance of the composite coating.

References

[1] LI H X, RUDNEV V S, ZHENG X H, YAROVAYA T P, SONG R G. Characterization of Al_2O_3 ceramic coating on 6063 aluminum alloy prepared in borate electrolytes by micro-arc oxidation [J]. J Alloys Comp, 2008, 462: 99−102.

[2] SUSAC D, SUN X, LI R Y, WONG K C, WONG P C, MITCHELL K A R, CHAMPANERIA R. Microstructural effects on the initiation of zinc phosphate coatings on 2024-T3 aluminum alloy [J]. Appl Surf Sci, 2004, 239: 45−59.

[3] KAUFFMANN F, JI B H, DEHM G, GAO H J, ARZT E. A quantitative study of the hardness of a superhard nanocrystalline titanium nitride/silicon nitride coating [J]. Scripta Materialia, 2005, 52: 1269−1274.

[4] MURATORE C, HU J J, VOEVODIN A A. Adaptive nanocomposite coatings with a titanium nitride diffusion barrier mask for high-temperature tribological applications [J]. Thin Solid Films, 2007, 515: 3638−3643.

[5] AZUSHIMA A, TANNO Y, IWATA H, AOKI K. Coefficients of friction of TiN coatings with preferred grain orientations under dry condition [J]. Wear, 2008, 265: 1017−1022.

[6] NAKATA K, USHIO M. Wear resistance of plasma sprayed Al-Si binary alloy coatings on A6063 Al alloy substrate [J]. Surf Coat Technol, 2001, 142/144: 277−282.

[7] GUI M, KANG S B. Aluminum hybrid composite coatings containing SiC and graphite particles by plasma spraying [J]. Materials Letters, 2001, 51: 396−401.

[8] WATANABE T, SATO T, NEZU A. Electrode phenomena investigation of wire arc spraying for preparation of Ti-Al intermetallic compounds [J]. Thin Solid Films, 2002, 407: 98−103.

[9] INGO G M, KACIULIS S, MEZZI A, VALENTE T, CASADEI F, GUSMANO G. Characterization of composite titanium nitride coatings prepared by reactive plasma spraying [J]. Electrochimica Acta, 2005, 50: 4531−4537.

[10] HSU C T, CHANG C C, CHANG T N, YEN S K. Electrolytic Al_2O_3/Y_2O_3 double-layer coating on IN617 superalloy [J]. Surf Coat Technol, 2006, 200: 6611−6617.

[11] SIAB R, BONNET G, BROSSARD J M, BALMAIN J, DINHUT J F. Effect of an electrodeposited yttrium containing thin film on the high-temperature oxidation behaviour of TA6V alloy [J]. Appl Surf Sci, 2007, 253: 3425−3431.

[12] WANG Wei, QIAN Shi-qiang, ZHOU Xi-ying, LIN Wen-song. Microstructure and properties of high speed jet electrodeposition nanocomposite coatings [J]. Transactions of Materials and Heat Treated, 2007, 28: 243−248.

[13] TAKEUCHI H, TAMURA S, TSUNEKAWA Y, OKUMIYA M. Application of electrolyte jet to rapid composite electroplating [J]. Surface Engineering, 2004, 20: 25−30.

[14] BHARATH R R, RAMANATHAN R, SUNDARARAJAN B, SRINIVASAN P B. Optimization of process parameters for deposition of stellite on X45CrSi93 steel by plasma transferred arc technique [J]. Mater Design, 2008, 29: 1725−1731.

[15] HUANG Z Y, HOU Q Y, WANG P. Microstructure and properties of Cr_3C_2-modified nickel-based alloy coating deposited by plasma transferred arc process [J]. Surf Coat Technol, 2008, 202: 2993−2999.

[16] DEUIS R L, SUBRAMANIAN C, YELLUP J M. Abrasive wear of composite coatings in a saline sand slurry environment [J]. Wear, 1997, 203/204: 119−128.

(Edited by YANG Bing)